Tsuda *et al. Earth, Planets and Space* (2018) 70:94
https://doi.org/10.1186/s40623-018-0864-y

Earth, Planets and Space

TECHNICAL REPORT

Open Access

Survey of conditions for artificial aurora experiments by the second electron gyro-harmonic at EISCAT Tromsø using dynasonde data

T. T. Tsuda[1*], M. T. Rietveld[2,3], M. J. Kosch[4,5,6], S. Oyama[7,8,9], Y. Ogawa[8,10], K. Hosokawa[1], S. Nozawa[7], T. Kawabata[7] and A. Mizuno[7]

Abstract

We report a brief survey of matching conditions for artificial aurora optical experiments utilizing the second electron gyro-harmonic (2.7-MHz frequency) in *F* region heating with O-mode at the EISCAT Tromsø site using dynasonde data from 2000 to 2017. Our survey indicates the following: The possible conditions for successful artificial aurora experiments are concentrated on twilight hours in both evening and morning, compared with late night hours; the possible conditions appear in fall, winter, and spring, while there is no chance in summer, and the month-to-month variation among fall, winter, and spring is not so clear; the year-to-year variation is well correlated with the solar activity. These characteristics in the case of 2.7-MHz frequency are basically similar to those previously reported in the case of 4-MHz frequency. However, the number of days meeting the possible condition in the case of 2.7-MHz frequency is obviously large, compared with that in the case of 4-MHz frequency. In particular, unlike the 4-MHz frequency operation, the 2.7-MHz frequency operation can provide many chances for successful artificial aurora experiments even during the solar minimum.

Keywords: Artificial aurora, Ionospheric heating, Second electron gyro-harmonic, EISCAT, Tromsø, Dynasonde

Background

A large number of ionospheric heating experiments using high-frequency (HF) radio waves have been performed by many researchers. A detailed overview on ionospheric heating experiments can be found in, e.g., Kosch et al. (2007a) and Leyser and Wong (2009). There are restrictions for successful heating experiments. A main restriction in artificial aurora experiments is that the ionospheric peak density drops below the lowest heater frequency too quickly after sunset. The weather condition is another important factor affecting the optical observations, but we do not treat the weather condition in the present study for simplicity. Due to such restrictions, some of heating experiments were successful (e.g., Gustavsson et al. 2005; Bryers et al. 2013; Kosch et al. 2005, 2007b, 2009, 2014a, b; Blagoveshchenskaya et al. 2015), but the others were unsuccessful. Thus, it is vitally important to understand when such successful conditions are likely satisfied for planning heating experiments in campaigns. However, such surveys are not sufficiently carried out.

Using observational data obtained by the dynasonde (Rietveld et al. 2008) at the European Incoherent SCATter (EISCAT) Tromsø site, Tsuda et al. (2018) carried out the first survey for artificial aurora experiments using *F* region heating with the ordinary mode (O-mode) by the EISCAT heating facility (Rietveld et al. 1993, 2016). In their survey, one of the required conditions for successful or possible artificial aurora experiments is that the *F* region critical frequency in O-mode (f_oF_2) is more than

*Correspondence: takuo.tsuda@uec.ac.jp
[1] Department of Computer and Network Engineering, The University of Electro-Communications (UEC), Chofu, Japan
Full list of author information is available at the end of the article

or equal to 4-MHz frequency, i.e., the minimum radio frequency of the present EISCAT heating system. This is because the electron energization by powerful O-mode HF waves, which lead to electron heating and optical emissions, can only occur when the radio frequency of transmitted HF waves is slightly lower than the maximum plasma frequency in the heating region. In addition, darkness is needed to observe the optical emissions, i.e., artificial aurora. Based on the survey, they suggested the following: The successful or possible conditions for the artificial aurora experiments are concentrated on twilight hours in both evening and morning, compared with late night hours; the possible conditions appear in fall, winter, and spring, while there is no chance in summer, and the month-to-month variation among fall, winter, and spring is not so clear; the year-to-year variation is well correlated with the solar activity, and experiments during the solar minimum would be almost hopeless. It should be noted that the plasma frequency is sufficiently high in summer but there is no chance in summer due to the lack of darkness at the high latitude, i.e., the EISCAT Tromsø site.

Another interest is a survey for artificial aurora experiments utilizing the second electron gyro-harmonic (e.g., Kosch et al. 2005, 2007b, 2009). Pumping the ionosphere in the second electron gyro-harmonic frequency is special, because on the second electron gyro-harmonic only there is a plasma resonance maximum. On all higher gyro-harmonic frequencies, there are plasma resonance minimums. The plasma resonance is found close to the gyro-frequency, but this is more difficult to achieve precisely because the ionosphere is not static, i.e., the plasma density varies and the height also varies, which varies the magnetic field strength. Thus, the frequency regime on the second electron gyro-harmonic allows more easily the study of various plasma instabilities (e.g., parametric decay instability for Langmuir, upper-hybrid, and electron Bernstein waves). Electron acceleration on the second gyro-harmonic is sufficiently intense that descending artificial ionization layers have been observed (e.g., Pedersen et al. 2010). The second gyro-harmonic frequency ($2f_{ce}$) can be calculated as: $2f_{ce} = 2 \times \frac{eB}{2\pi m}$. Here, e is the elementary charge (1.602×10^{-19} C), m is the electron mass (9.109×10^{-31} kg), and B is the ionospheric magnetic field strength which is roughly 47,000–49,000 nT at 200–300 km heights above the EISCAT Tromsø site. Hence, the second electron gyro-harmonic frequency is roughly 2.6–2.7 MHz. Thus, in the present paper, we present a survey of conditions for artificial aurora experiments by 2.7-MHz frequency, i.e., the second electron gyro-harmonic frequency, at the EISCAT Tromsø site using dynasonde data. This is an extension to the survey of Tsuda et al. (2018). The information obtained in this survey provides a strong scientific basis to re-introduce a low-frequency capability to the EISCAT heating facility. It should be mentioned that originally the EISCAT heating facility was able to transmit between 2.7 and 4 MHz from 1980 until October 1985 when a storm catastrophically damaged the low-frequency antennas. That antenna array was rebuilt for higher frequencies, but a limited modification for low frequencies may be feasible (see Rietveld et al. 2016).

Methods

The present survey is basically the same as that employed by Tsuda et al. (2018), but for the case of 2.7-MHz frequency (i.e., for the artificial aurora experiments utilizing the second electron gyro-harmonic). For a statistical survey, we accumulated f_oF_2 data from 2000 to 2017 (precisely to 06:06 UT on October 11, 2017), obtained by the dynasonde at the EISCAT Tromsø site (69.6°N, 19.2°E). The data period covers more than one solar cycle. A sounding was made typically every 6 minutes before February 2012 and every 2 minutes since then. Using the dataset, we categorized each period of 1 h into three conditions: (a) possible nighttime heating condition; (b) impossible nighttime heating condition; and (c) no data. To judge the conditions, we set four criteria: (1) number of f_oF_2 data for each 1-h period is at least 5; (2) averaged f_oF_2 for each period of 1 h is more than or equal to 2.7 MHz; (3) one standard deviation of f_oF_2 for each period of 1 h is less than or equal to 0.5 MHz; (4) minimum of solar zenith angle (SZA) for each period of 1 h is more than or equal to 96°. If the criterion (1) is not satisfied, the 1 h is categorized as the condition (c). If all the criteria are satisfied, the 1 h is categorized as the condition (a). Otherwise, the 1 h is categorized as the condition (b). Note that the criterion (2) is for O-mode heating in the second electron gyro-harmonic, the criterion (3) is for stable ionosphere or stable heating which would be important for, e.g., ON–OFF heating operation, and the criterion (4) is for nighttime including both the nautical twilight and the astronomical twilight to detect optical emissions, i.e., artificial aurora emissions.

Results and discussion

Local time variation

Figures 1, 2, 3 show UT-date variations in the possibility for the artificial aurora experiments from 2000 to 2017. It seems that the possible hours are fairly concentrated around the evening hours, i.e., a few hours after sunset, compared with the late night hours. Another interesting characteristic is that a number of the possible hours can be found in the morning hours, i.e., a few hours before sunrise. These would indicate that relatively high electron density can be maintained at twilight hours due to

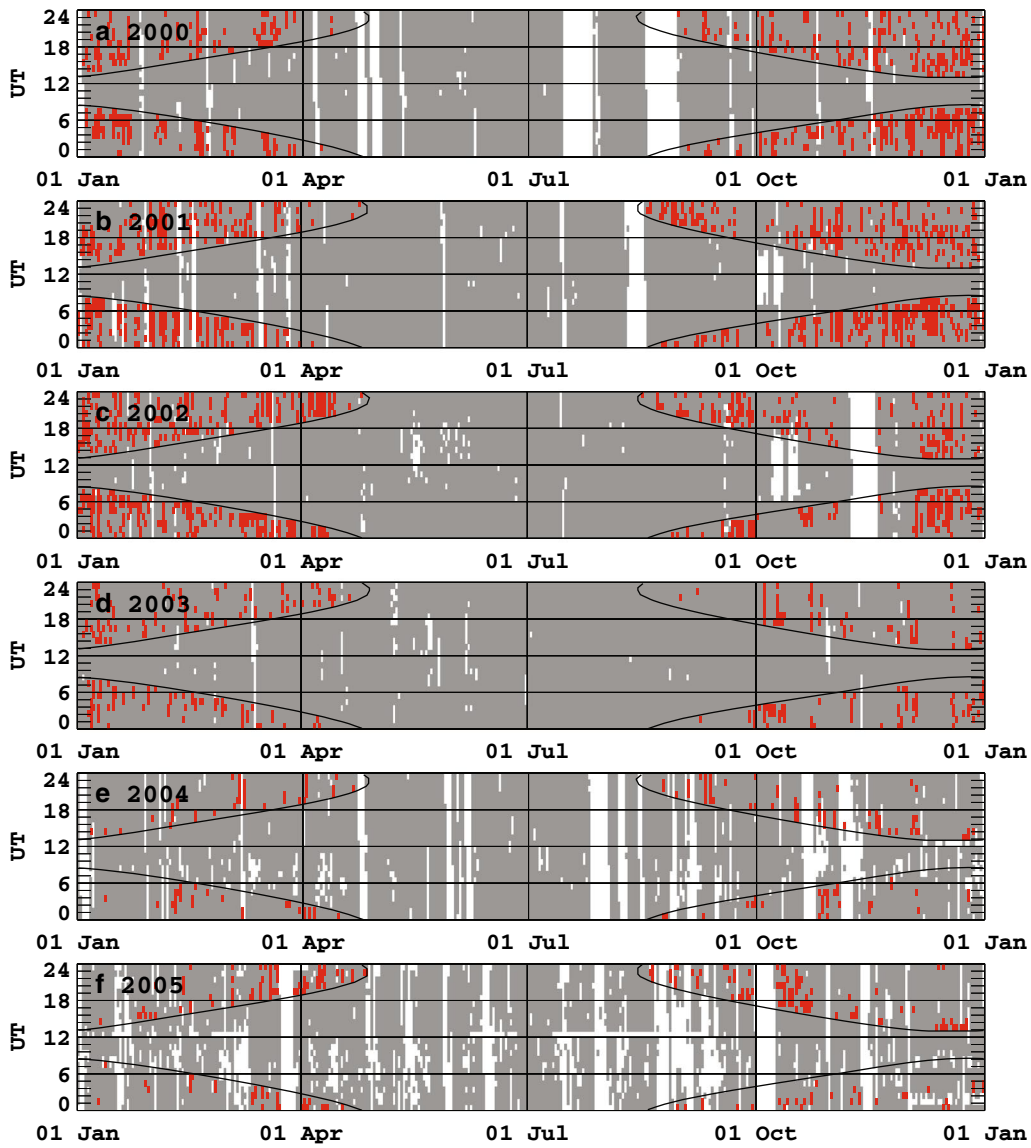

Fig. 1 Variations in possible UT-date for conducting artificial aurora experiments from 2000 to 2005 (from **a** to **f**). The red region indicates periods under the possible condition, and the gray region indicates periods under the impossible condition. The white region corresponds to periods when there are no data. The solar zenith angle (SZA) of 96° is described by the black curve. Note that LT = UT + 1 h (for winter time), at Tromsø

solar illumination in the F region. These characteristics are basically similar to those by Tsuda et al. (2018), but the number of the possible hours seems to be large, compared with that by Tsuda et al. (2018). This would be due to the change in the criterion (2) (i.e., 4–2.7 MHz in the averaged f_oF_2).

Month-to-month variation

To see seasonal variation in detail, Figs. 4, 5, 6 show month-to-month variations of the number of days for possible artificial aurora experiments from 2000 to 2017. Here, if there are no data in a day, we define the day as no data, marked by black. If there is the possible condition of at least 1 h in a day, we define the day as the possible condition, marked by red. Otherwise, we define the day as the impossible condition, marked by gray. Obviously, there was no chance for the possible condition during summer, i.e., roughly May to July. This is because the criterion (4) for nighttime condition is never satisfied during the summer. On the other hand, we can find the possible condition from August to April, i.e., fall, winter, and spring. Of particular interest, we can find that there

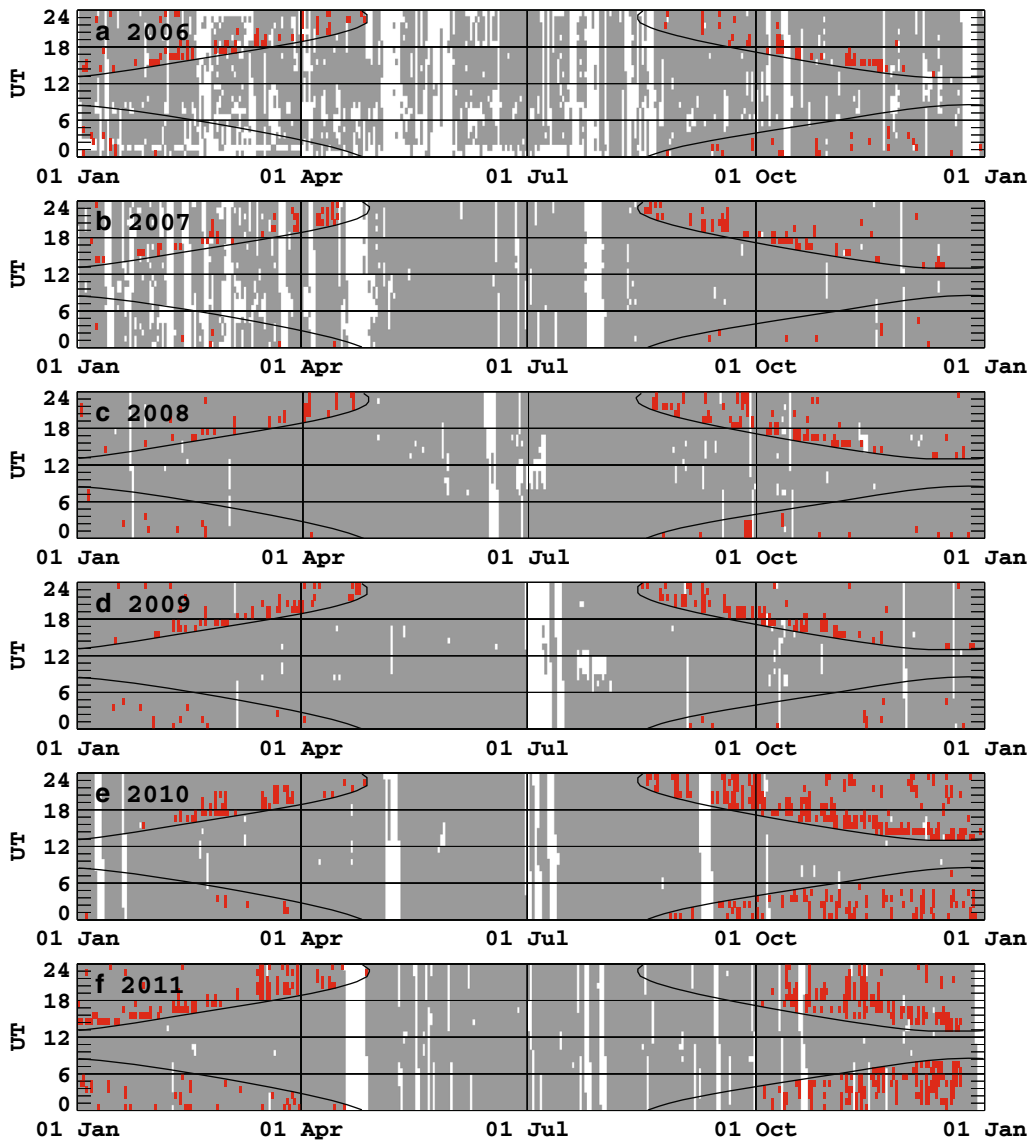

Fig. 2 Variations in possible UT-date for conducting artificial aurora experiments from 2006 to 2011 (from **a** to **f**). The red region indicates periods under the possible condition, and the gray region indicates periods under the impossible condition. The white region corresponds to periods when there are no data. The solar zenith angle (SZA) of 96° is described by the black curve. Note that LT = UT + 1 h (for winter time), at Tromsø

were many chances for the artificial aurora experiments in winter. It seems that the number of days in the possible condition during winter is not much smaller than or is similar to those during spring as well as fall. Generally, there should be differences in the solar irradiation between winter and spring/fall. Such seasonal differences would be mainly due to different SZAs. However, in the twilight hours, the SZA should be roughly the same in any season. Hence, relatively high electron density can be maintained in the illuminated F region during the twilight hours in any season. This would be a reason for the observed unclear seasonal variation. Again, these characteristics are basically similar to those in Tsuda et al. (2018), but the number of the possible days seems to be large, compared with that in Tsuda et al. (2018).

Year-to-year variation

Figure 7 shows year-to-year variations of the number of days with the possibility for the artificial aurora experiments from 2000 to 2017, with 1-year average of the solar radio flux index at 10.7 cm (2800 MHz), $F_{10.7}$. Note that the averaged $F_{10.7}$ in 2017 is calculated using

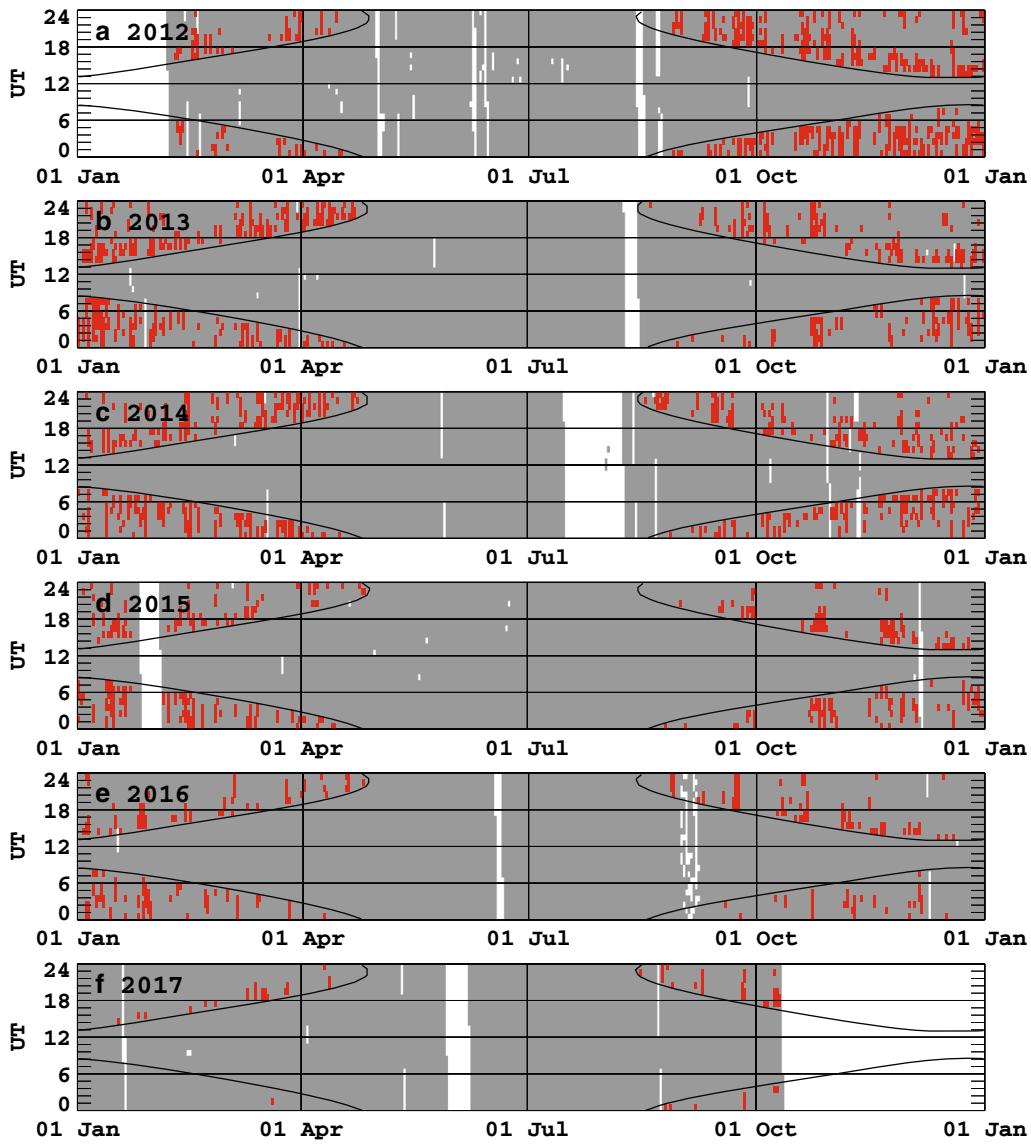

Fig. 3 Variations in possible UT-date for conducting artificial aurora experiments from 2012 to 2017 (from **a** to **f**). The red region indicates periods under the possible condition, and the gray region indicates periods under the impossible condition. The white region corresponds to periods when there are no data. The solar zenith angle (SZA) of 96° is described by the black curve. Note that LT = UT + 1 h (for winter time), at Tromsø

data to August 31, 2017. We can find a clear relationship between the averaged $F_{10.7}$ and the number of days in the possible condition in the case of 2.7-MHz frequency (see Fig. 7a). This characteristic is similar to that in the case of 4-MHz frequency (see Fig. 7b) by Tsuda et al. (2018). However, the number of the possible days during the solar minimum was obviously large, compared with that in the case of 4-MHz frequency. In Fig. 7c, we compare occurrence rates in the possible days for the artificial aurora experiments in the cases of 2.7- and 4-MHz frequencies. For example, during 2006–2009 (i.e., the solar minimum), the occurrence rates were very low (1–2%) in the case of 4-MHz frequency [i.e., in the survey by Tsuda et al. (2018)], while those were 24–30% in the case of 2.7-MHz frequency (i.e., in the present survey).

Thus, the results indicate that in the case of 2.7-MHz frequency there are many chances for the artificial aurora experiments even during the solar minimum. This would be a big advantage in the 2.7-MHz frequency operation. So, if an upgrade to the 2.7-MHz frequency operation in the EISCAT heating facility is realized, chances for the artificial aurora experiments can be much enhanced even

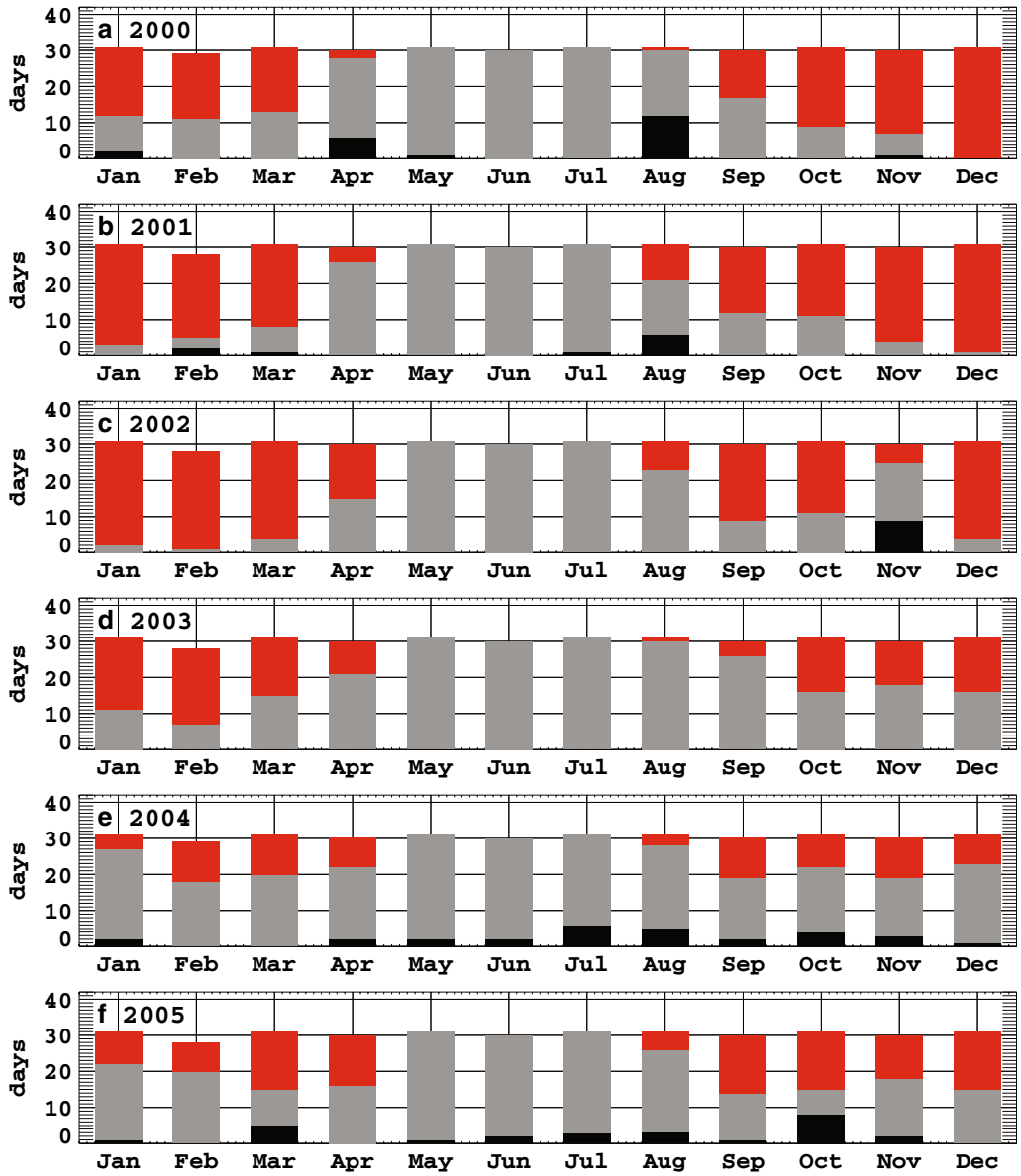

Fig. 4 Month-to-month variations of the number of possible days for conducting artificial aurora experiments from 2000 to 2005 (from **a** to **f**). The red bars indicate the possible days, while the gray bars indicate days in which conducting the experiments is not possible, and the black bars indicate days when there are no data

during the solar minimum. This means that we do not have to wait for the next solar maximum, i.e., the maximum of the cycle 25, which would be 2022–2023 according to solar cycle predictions (e.g., Rigozo et al. 2011; Attia et al. 2013; Li et al. 2015). In addition, there would be much new science related to the second electron gyro-harmonic (e.g., various plasma instabilities such as parametric decay instability for Langmuir, upper-hybrid, and electron Bernstein waves).

Historically, the EISCAT heating facility could operate around the second electron gyro-harmonic frequency (2.76 MHz) in the early 1980s (e.g., Frey 1986), but this

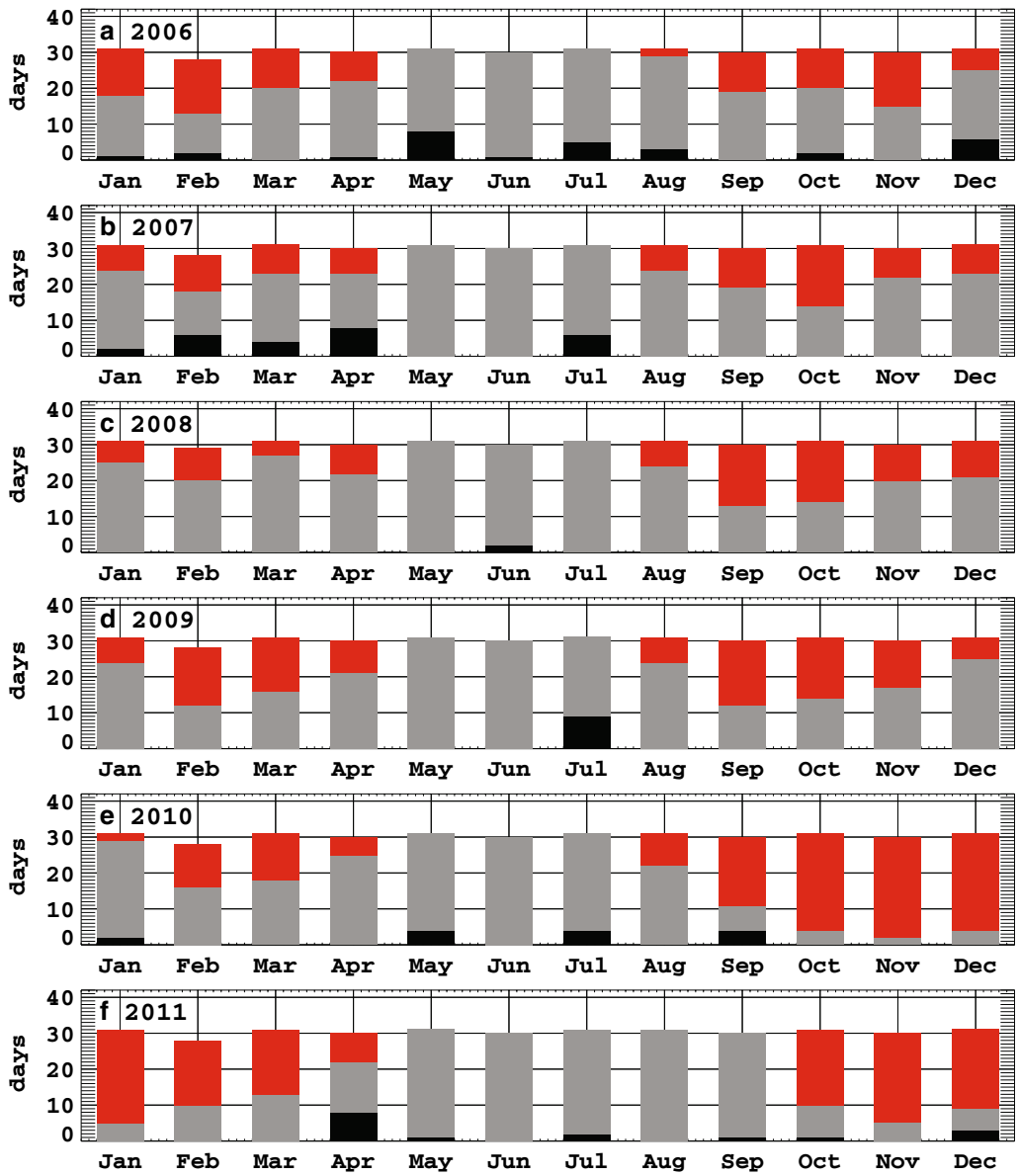

Fig. 5 Month-to-month variations of the number of possible days for conducting artificial aurora experiments from 2006 to 2011 (from **a** to **f**). The red bars indicate the possible days, while the gray bars indicate days in which conducting the experiments is not possible, and the black bars indicate days when there are no data

capability was not fully exploited then because of a lack of advanced diagnostic instruments and radar techniques available at that time. The HIgh-Power Auroral Stimulation (HIPAS) also had a capability of the operation for the second electron gyro-harmonic frequency, but HIPAS stopped operating in 2007. The High-frequency Active Auroral Research Program (HAARP) can be used for the second electron gyro-harmonic frequency operation, but there is no incoherent scatter radar near the HAARP. EISCAT has two incoherent scatter radars colocated with the EISCAT heating facility, which would be a huge advantage if the EISCAT heating facility could get the 2.7-MHz capability back. Later, EISCAT_3D will also be a valuable diagnostic for a 2.7-MHz heating

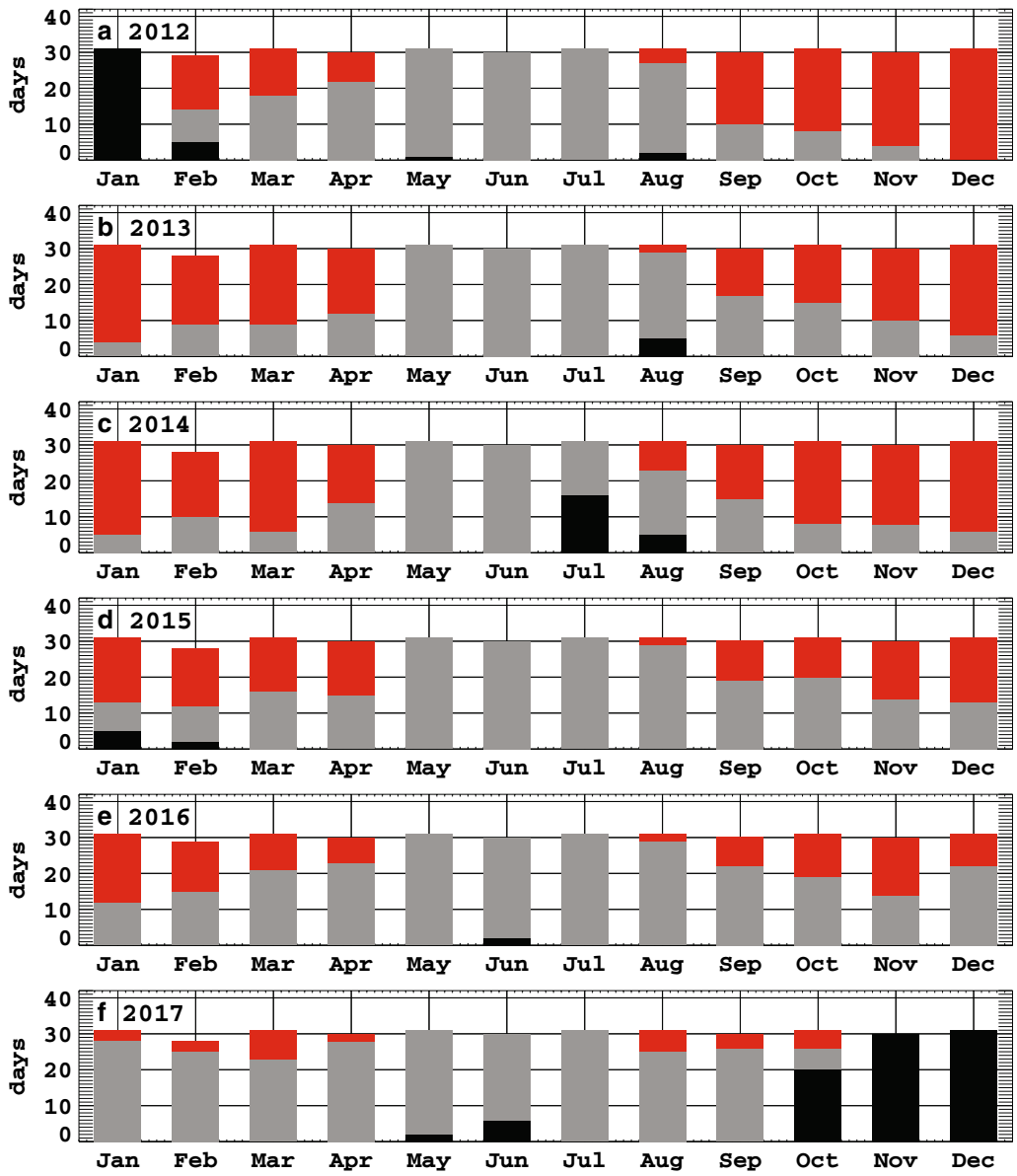

Fig. 6 Month-to-month variations of the number of possible days for conducting artificial aurora experiments from 2012 to 2017 (from **a** to **f**). The red bars indicate the possible days, while the gray bars indicate days in which conducting the experiments is not possible, and the black bars indicate days when there are no data

facility. EISCAT_3D and the heating facility will not be colocated, but EISCAT_3D will be able to cover the ionosphere above the heating facility at Tromsø. Thus, we will be able to perform multi-point observations along the local magnetic field line at heating facility with multiple beams by EISCAT_3D.

Conclusions

We carried out a statistical survey of conditions for artificial aurora experiments by 2.7-MHz frequency at EISCAT Tromsø site using dynasonde data from 2000 to 2017. This survey is an extended work of the survey in the case of 4-MHz frequency by Tsuda et al. (2018). Local time, month-to-month, and year-to-year variations in the possibility for the artificial aurora experiments by 2.7-MHz frequency are generally similar to those in the case of 4-MHz frequency. However, the number of days with the right ionospheric condition in the case of 2.7-MHz frequency was obviously much larger, compared with that in the case of 4-MHz frequency. In particular, in

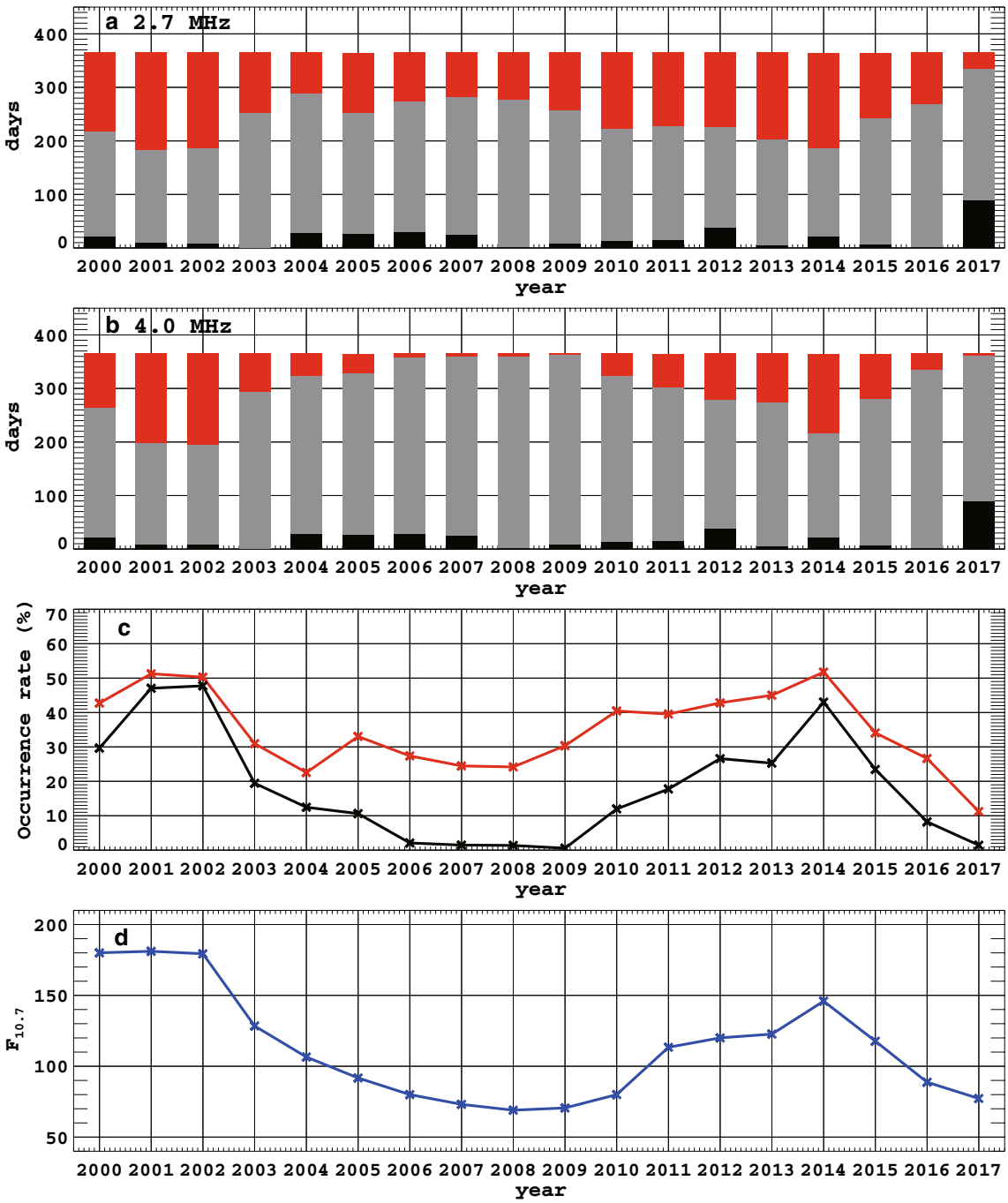

Fig. 7 **a** Year-to-year variations in the number of possible days for conducting artificial aurora experiments from 2000 to 2017, in the case of 2.7-MHz frequency. The red bars indicate possible days, the gray bars indicate days in which conducting the experiments is not possible, and the black bars indicate days when there are no data. **b** Same as **a**, but in the case of 4-MHz frequency (Tsuda et al. 2018). **c** Year-to-year variation in the occurrence rate of possible days for conducting artificial aurora experiments from 2000 to 2017. The red indicates results in the case of 2.7-MHz frequency, and the black indicates results in the case of 4-MHz frequency. **d** Year-to-year variation in 1-year-averaged $F_{10.7}$ from 2000 to 2017

the case of 2.7-MHz frequency, unlike the case of 4-MHz frequency, there would be many chances for the artificial aurora experiments even during the solar minimum. This would be an important advantage in the 2.7-MHz frequency operation by the EISCAT heating facility, if it become a reality in the future.

Abbreviations
EISCAT: European Incoherent SCATter; HAARP: high-frequency active auroral research program; HF: high frequency; HIPAS: high-power auroral stimulation; LT: local time; O-mode: ordinary mode; SD: standard deviation; SZA: solar zenith angle; UT: universal time.

Authors' contributions
TTT conducted data analysis and wrote the first draft of the manuscript. MTR accumulated the dataset by operating the dynasonde and supported the data analysis. MJK, SO, YO, KH, SN, TK, and AM contributed toward interpreting the results. All authors have contributed toward revising and improving the manuscript. All authors have read and approved the final manuscript.

Author details
[1] Department of Computer and Network Engineering, The University of Electro-Communications (UEC), Chofu, Japan. [2] European Incoherent SCATter (EISCAT) Scientific Association, Tromsø, Norway. [3] Department of Physics and Technology, University of Tromsø (UiT) - The Arctic University of Norway, Tromsø, Norway. [4] South African National Space Agency (SANSA), Hermanus, South Africa. [5] Department of Physics, Lancaster University, Lancaster, UK. [6] Department of Physics and Astronomy, University of the Western Cape, Bellville, South Africa. [7] Institute for Space-Earth Environmental Research (ISEE), Nagoya University, Nagoya, Japan. [8] National Institute of Polar Research (NIPR), Tachikawa, Japan. [9] Ionosphere Research Unit, University of Oulu, Oulu, Finland. [10] Department of Polar Science, Graduate University for Advanced Studies (SOKENDAI), Tachikawa, Japan.

Acknowledgements
We thank European Incoherent SCATter (EISCAT) scientific association for providing dynasonde data. EISCAT is an international association supported by research organizations in China (CRIRP), Finland (SA), Japan (NIPR), Norway (NFR), Sweden (VR), and the UK (NERC). The dynasonde data can be available on request to M. T. Rietveld (mike@eiscat.uit.no) or can be accessed directly at the website, EISCAT Dynasonde (http://dynserv.eiscat.uit.no/DD/login.php). The 10.7-cm solar radio flux index data, $F_{10.7}$ data, are provided at the Web site, National Centers for Environmental Information (NCEI), National Oceanic and Atmospheric Administration (NOAA) (ftp://ftp.ngdc.noaa.gov/STP/GEOMAGNETIC_DATA/INDICES/KP_AP). This work was supported in part by MEXT/JSPS KAKENHI grants, JP26610157, JP15H05747, JP15H05815, JP16H01171, JP16H02230, JP16H06021, JP16H06286, JP16K05569, and JP17H02968, by the Sumitomo Foundation Basic Science Research grant, 150627, by National Institute of Polar Research (NIPR) through General Collaboration Project, 28-2, and by the joint research program of the Institute for Space-Earth Environmental Research (ISEE), Nagoya University.

Competing interests
The authors declare that they have no competing interests.

Ethics approval and consent to participate
Not applicable.

Publisher's Note

Received: 26 February 2018 Accepted: 16 May 2018
Published online: 06 June 2018

References
Attia AF, Ismail HA, Basurah HM (2013) A Neuro-Fuzzy modeling for prediction of solar cycles 24 and 25. Astrophys Space Sci 344:5–11. https://doi.org/10.1007/s10509-012-1300-6

Blagoveshchenskaya NF, Borisova TD, Kosch M, Sergienko T, Brändström U, Yeoman TK, Häggström I (2015) Optical and ionospheric phenomena at EISCAT under continuous X-mode HF pumping. J Geophys Res Space Phys 119:10483–10498. https://doi.org/10.1002/2014JA020658

Bryers CJ, Kosch MJ, Senior A, Rietveld MT, Singer W (2013) A comparison between resonant and nonresonant heating at EISCAT. J Geophys Res Space Phys 118:6766–6776. https://doi.org/10.1002/jgra.50605

Frey A (1986) The observation of HF-enhanced plasma waves with the EISCAT/UHF-radar in the presence of strong Landau-damping. Geophys Res Lett 13:438–441. https://doi.org/10.1029/GL013i005p00438

Gustavsson B, Sergienko T, Kosch MJ, Rietveld MT, Brändström BUE, Leyser TB, Isham B, Gallop P, Aso T, Ejiri M, Grydeland T, Steen Å, LaHoz C, Kaila K, Jussila J, Holma H (2005) The electron energy distribution during HF pumping, a picture painted with all colors. Ann Geophys 23:1747–1754. https://doi.org/10.5194/angeo-23-1747-2005

Kosch MJ, Pedersen T, Hughes J, Marshall R, Gerken E, Senior A (2005) Artificial optical emissions at HAARP for pump frequencies near the third and second electron gyro-harmonic. Ann Geophys 23:1585–1592. https://doi.org/10.5194/angeo-23-1585-2005

Kosch MJ, Pedersen T, Rietveld MT, Gustavsson B, Grach SM, Hagfors T (2007a) Artificial optical emissions in the high-latitude thermosphere induced by powerful radio waves: an observational review. Adv Space Res 40:365–376. https://doi.org/10.1016/j.asr.2007.02.061

Kosch MJ, Pedersen T, Mishin E, Oyama S, Hughes J, Senior A, Watkins B, Bristow B (2007b) Coordinated optical and radar observations of ionospheric pumping for a frequency pass through the second electron gyroharmonic at HAARP. J Geophys Res 112:A06325. https://doi.org/10.1029/2006JA012146

Kosch MJ, Gustavsson B, Heinselman C, Pedersen T, Rietveld MT, Spaleta J, Wong A, Wang W, Mutiso C, Bristow B, Hughes J (2009) First incoherent scatter radar observations of ionospheric heating on the second electron gyro-harmonic. J Atmos Sol Terr Phys 71:1959–1966. https://doi.org/10.1016/j.jastp.2009.08.007

Kosch MJ, Vickers H, Ogawa Y, Senior A, Blagoveshchenskaya N (2014) First observation of the anomalous electric field in the topside ionosphere by ionospheric modification over EISCAT. Geophys Res Lett 41:7427–7435. https://doi.org/10.1002/2014GL061679

Kosch MJ, Bryers C, Rietveld MT, Yeoman TK, Ogawa Y (2014) Aspect angle sensitivity of pump-induced optical emissions at EISCAT. Earth Planets Space 66:159. https://doi.org/10.1186/s40623-014-0159-x

Leyser TB, Wong AY (2009) Powerful electromagnetic waves for active environmental research in geospace. Rev Geophys 47:RG1001. https://doi.org/10.1029/2007RG000235

Li KJ, Feng W, Li FY (2015) Predicting the maximum amplitude of solar cycle 25 and its timing. J Atmos Sol Terr Phys 135:72–76. https://doi.org/10.1016/j.jastp.2015.09.010

Pedersen T, Gustavsson B, Mishin E, Kendall E, Mills T, Carlson HC, Snyder AL (2010) Creation of artificial ionospheric layers using high-power HF waves. Geophys Res Lett 37:L02106. https://doi.org/10.1029/2009GL041895

Rietveld MT, Kohl H, Kopka H, Stubbe P (1993) Introduction to ionospheric heating at Tromsø—I. Experimental overview. J Atmos Terr Phys 55:577–599. https://doi.org/10.1016/0021-9169(93)90007-L

Rietveld MT, Wright JW, Zabotin N, Pitteway MLV (2008) The Tromsø dynasonde. Polar Sci 2:55–71. https://doi.org/10.1016/j.polar.2008.02.001

Rietveld MT, Senior A, Markkanen J, Westman A (2016) New capabilities of the upgraded EISCAT high-power HF facility. Radio Sci 51:1533–1546. https://doi.org/10.1002/2016RS006093

Rigozo NR, Souza Echer MP, Evangelista H, Nordemann DJR, Echer E (2011) Prediction of sunspot number amplitude and solar cycle length for cycles 24 and 25. J Atmos Sol Terr Phys 73:1294–1299. https://doi.org/10.1016/j.jastp.2010.09.005

Tsuda TT, Rietveld MT, Kosch MJ, Oyama S, Hosokawa K, Nozawa S, Kawabata T, Mizuno A, Ogawa Y (2018) Survey of conditions for artificial aurora experiments at EISCAT Tromsø using dynasonde data. Earth Planets Space 70:40. https://doi.org/10.1186/s40623-018-0805-9